

Carrier multiplication yields of CdSe and CdTe nanocrystals by transient photoluminescence spectroscopy

Gautham Nair and Mounqi G. Bawendi*

Department of Chemistry, Massachusetts Institute of Technology, 77 Massachusetts Avenue, Cambridge, Massachusetts 02139, USA

(Received 17 July 2007; published 13 August 2007)

Engineering semiconductors to enhance carrier multiplication (CM) could lead to increased photovoltaic cell performance and a significant widening of the materials range suitable for future solar technologies. Semiconductor nanocrystals (NCs) have been proposed as a favorable structure for CM enhancement, and recent measurements by transient absorption have shown evidence for highly efficient CM in lead chalcogenide and CdSe NCs. We report here an assessment of CM yields in CdSe and CdTe NCs by a quantitative analysis of biexciton and exciton signatures in transient photoluminescence decays. Although the technique is particularly sensitive due to enhanced biexciton radiative rates relative to the exciton, $k_{BX}^{\text{rad}} > 2k_X^{\text{rad}}$, we find no evidence for CM in CdSe and CdTe NCs up to photon energies $\hbar\omega > 3E_g$, well above previously reported relative energy thresholds.

DOI: 10.1103/PhysRevB.76.081304

PACS number(s): 78.55.Et, 73.22.Dj, 73.90.+f, 78.67.Bf

Carrier multiplication (CM) in the form of impact ionization is a well-understood phenomenon in bulk semiconductors.^{1,2} The process, consisting of inelastic scattering of energetic charge carriers and valence electrons to create additional e - h pairs, normally has high energy thresholds and low efficiency due to momentum conservation requirements and competition from ultrafast intraband relaxation. While this conventional bulk CM has found a particular application in avalanche photodiodes for single photon detection, efficient CM following optical excitation could have a significantly wider impact in the area of solar energy conversion.

In a typical photovoltaic cell with a single active layer, photon energy in excess of the band gap is lost by rapid thermalization. The CM process, if efficient, could harvest this excess energy into additional e - h pairs, boosting the maximum theoretical power conversion efficiency from 32% to >40%,^{3,4} and, more importantly, widening the range of candidate materials for new solar technologies to include previously ignored narrow-gap semiconductors. Strongly confined semiconductor nanocrystals (NCs) have been proposed as candidate structures for efficient CM (Ref. 5) because of an anticipated relaxation of momentum conservation constraints^{6,7} and potential slowing of competing phonon-mediated intraband cooling due to the discrete electronic structure (“phonon bottleneck”).⁵

Recently, transient absorption (TA) measurements have shown evidence of efficient ultrafast CM in ir-emitting PbSe, PbS, and PbTe NCs above a photon energy threshold $\hbar\omega = 3E_g$.^{8–10} In extensions of the work, subsequent TA measurements have indicated that a single photon could generate up to seven e - h pairs in PbSe (Ref. 11) and that CM is similarly efficient in visible-emitting CdSe NCs above a $\hbar\omega = 2.5E_g$ threshold.¹²

The conclusions of the TA measurements suggest new and unique underlying physics as well as some interesting questions. First-principles theories explaining the balance of Coulomb coupling and phonon relaxation rates implied by the experiments have yet to emerge. At the same time, studies on intraband relaxation in CdSe and PbSe NCs at room temperature have found fast cooling dynamics that do not appear

consistent with a phonon bottleneck.^{13–15} In addition, some aspects of the experimental data are intriguing, such as similar CM effects seen in PbSe and CdSe despite the very different state structures at threshold, and the observed linear dependence of CM yields on excess energy.¹²

We present here an assessment of CM yields in CdSe and CdTe nanocrystals by transient photoluminescence (tPL). While complementary to TA in some ways, tPL is a background-free measurement better suited to the low excitation fluences necessary in CM studies. It is also more selective since it relates to the number of e - h pairs instead of single-particle state filling. Both TA and tPL capitalize on the unique, fast dynamics of multiexciton (MX) states^{16–18} to isolate and quantify MX populations, and though more complicated to interpret, tPL becomes a useful and particularly sensitive technique when carefully calibrated. A recent study has analyzed CM yields in CdSe NCs by tPL and concludes that there is agreement with previous TA determinations.¹⁹ Their analysis and experiment differs from ours in several significant ways. We find instead that CM efficiency in CdSe and CdTe NCs is close to zero even for photon energies up to $3.1E_g$. Implications are discussed.

Tunable uv excitation pulses were generated by nonlinear mixing of the visible output and 3.1 eV remnant of an optical parametric amplifier (Coherent OPA 9400) pumped by a 250 kHz amplified Ti:sapphire laser (Coherent RegA 9000). In a separate experiment, the Ti:sapphire was tuned to the red and 5.9 eV pulses were obtained by doubling its second harmonic. Room temperature hexane dispersions of NCs in 1 mm-path-length cuvettes were excited at 45° incidence. Emission was collected front-face and spectrally dispersed onto a streak camera (Hamamatsu C5680). We studied both organic ligand-capped CdSe or CdTe (core) and CdSe/ZnS or CdSe/ZnCdS (core/shell) overcoated particles.³¹

Figure 1 shows PL decays of a representative sample of $E_g = 2.0$ eV CdSe NCs under weak and strong excitation at 3.1 eV and 5.6 eV (E_g determined from the lowest absorption feature). At high fluence both decays show an additional fast component consistent with biexciton (BX) emission. Remarkably, and unlike data from Ref. 19 which shows a fast

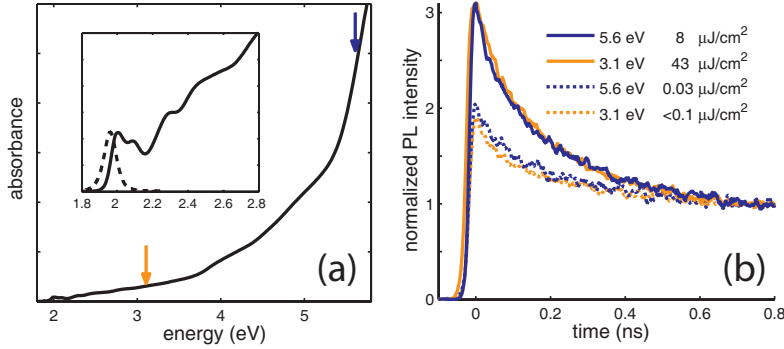


FIG. 1. (Color online). (a) Absorption spectrum of a typical CdSe NC core sample used. Excitation energies employed in tPL are indicated by the arrows. (Inset) Detail of band edge absorption structure and emission spectrum. (b) Band edge luminescence dynamics of the sample at the two indicated excitation energies for peak pulse fluence as noted.

component under uv excitation, we find that the two low-fluence decays follow each other closely, suggesting that CM is less efficient than previously reported. A quantitative determination of the CM yield requires first a careful characterization of the BX tPL signature, which we describe in detail.

Results of an excitation-fluence series at 3.1 eV are shown in Fig. 2. Decays at low fluence are dominated by exciton (X) emission. In most cases, X dynamics are multiexponential with contributions from NCs with different nonradiative relaxation and trapping rates.^{20,21} The decays are adequately described by a biexponential, $f(t) = \exp(-t/\tau_{Xslow}) + c_{fast} \exp(-t/\tau_{Xfast})$, chosen for simplicity, where $\tau_{Xfast} \approx 100$ – 300 ps and $\tau_{Xslow} \approx 1$ – 10 ns. With increasing fluence, early-time spectra show BX emission at the band edge and a further, blueshifted feature corresponding to $1P$ - $1P$ emission from higher multiexcitons [Figs. 2(a) and 2(b)].^{17,18} The BX state then decays quickly with a size-dependant lifetime $\tau_{BX} \approx 0.1$ – 1 ns due to a fast nonradiative “Auger”-like Coulomb process.¹⁶ As shown in Fig. 2(c), the measured tPL decays are well described by a superposition of X dynamics and an additional single exponential BX component, $a_{BX} \exp(-t/\tau_{BX}) + a_X f(t)$.

The relationship between the observed tPL decay amplitudes, a_X and a_{BX} , and the underlying MX populations was studied using a first-order kinetic model of MX relaxation, $p'_m(t) = -k_m p_m + k_{m+1} p_{m+1}$, giving $a_X \propto p_{m>0}^o k_X^{rad}$ and

$$a_{BX} \propto p_{m>1}^o (k_{BX}^{rad} - k_X^{rad}) \left(1 + \frac{k_2}{k_3 - k_2} \frac{p_{m>2}^o}{p_{m>1}^o} + \dots \right),$$

where p_m is the relative population of NCs with m electrons and holes, p_m^o are initial values at $t=0$, k_m are the MX decay rates, and k_X^{rad} and k_{BX}^{rad} are the X and BX radiative rates. The a_{BX} term includes BX populations formed by cascaded decay of higher MX states and is proportional to $k_{BX}^{rad} - k_X^{rad}$ since BX emission is partially offset by correspondingly reduced X emission at early times.³¹ The p_m^o are related to the incident laser power assuming poissonian photon absorption statistics and explicitly accounting for the inhomogeneous excitation profile of the beam,

$$p_m^o = \int \frac{n(\vec{r})^m}{m!} e^{-n(\vec{r})} d^3\vec{r}, \quad n(\vec{r}) = j_p(\vec{r})\sigma,$$

where $j_p(\vec{r})$ is the measured photon flux at \vec{r} , $n(\vec{r})$ is the average number of absorbed photons per NC, and σ is the

absorption cross section, treated here as an adjustable parameter.

Band edge PL decays show growth and slow saturation of a_X and a_{BX} that fit reasonably well to the expected curves [see Fig. 2(d)].³² From the fits we extract the a_{BX}/a_X ratio expected at BX saturation ($p_{m=2}^o = p_{m>0}^o$) and find a sample-dependant (a_{BX}/a_X)_{sat} value in the range 3–6. This implies a substantially faster radiative rate of the BX relative to the X and leads to enhanced sensitivity of tPL for detection of small multiexciton populations, as is illustrated by the prominence of BX features in Fig. 2(c). We estimate $k_{BX}^{rad}/k_X^{rad} > 3$ – 5 , consistent with previous measurements on high quality NCs showing $k_{BX}^{rad}/k_X^{rad} \approx 3$.²²

The observed faster radiative lifetime of the BX relative to the X is explained by the electronic fine structure of these states. Because emission from the X ground state is

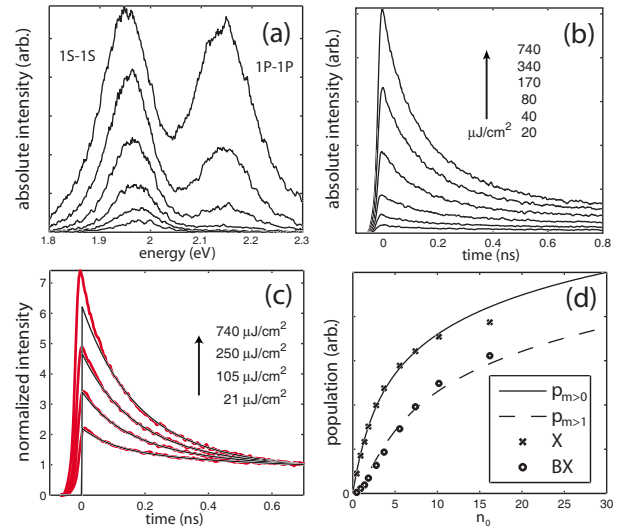


FIG. 2. (Color online) (a) Transient PL spectra of the NCs in Fig. 1 collected from $t=-10$ ps to $t=10$ ps and (b) decays integrated from 1.89 to 2.02 eV under 3.1 eV excitation with peak fluences as noted. (c) A separate subset of our data, showing PL decays normalized at long times. The black lines are fits to the form $a_{BX} e^{-t/\tau_{BX}} + a_X f(t)$ where $\tau_{BX} = 185$ ps and $f(t)$, the single X dynamics, are kept constant (Refs. 30 and 31). (d) (Lines) Predicted initial NC populations in an X or higher state ($p_{m>0}$) or in a BX or higher state ($p_{m>1}$) plotted against the peak average number of e - h pairs created, $n_0 = \max\{n(\vec{r})\}$. (\times , \circ) Scaled and fit a_X and a_{BX} PL components extracted from fits to measured decays.

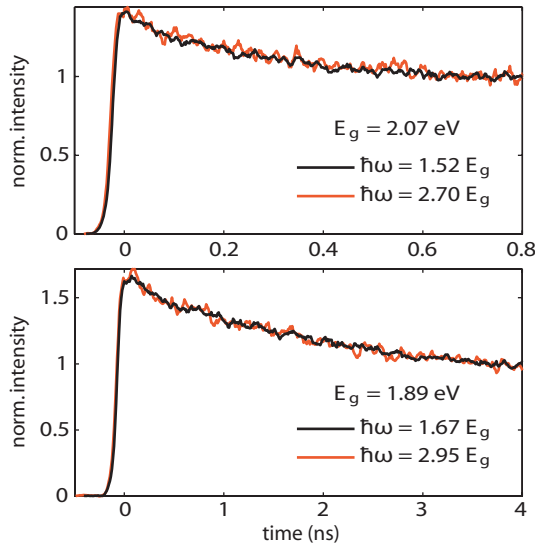


FIG. 3. (Color online) Band edge PL decays of $E_g=2.07$ eV (top) and $E_g=1.89$ eV (bottom) core/shell CdSe NCs under weak ($n_0 < 0.01$) excitation at 3.1 eV (black) and 5.6 eV (red). The 5.6 eV excitation corresponds to $\hbar\omega=2.70E_g$ and $2.95E_g$, respectively, for which TA measurements at 6.2 eV predict CM yields of 22% and 50% (Ref. 12).

spin forbidden, X luminescence is relatively slow ($k_X^{\text{rad}} \approx 0.05 \text{ ns}^{-1}$) and consists mostly of emission from thermally populated spin-allowed bright states.^{23–25} However, transitions from the BX ground state to some states in the X fine structure are predicted to be optically allowed,²⁵ indicating that k_{BX}^{rad} can be significantly larger than the $2k_X^{\text{rad}}$ value one would predict from a simple carrier counting argument.

The sensitivity of the tPL experiment was thus exploited to estimate carrier multiplication yields in NC samples under uv excitation.³³ We find that, while signatures of multiexciton emission appear at high fluence, decays under weak 5.6 or 5.9 eV excitation are close to indistinguishable from decays under weak 3.1 eV (Fig. 3) even for large NCs where the excitation energy $\hbar\omega$ exceeds $3E_g$. This contrasts with the measurements of Ref. 19 which show an additional fast component under uv excitation. Quantitative values shown in Fig. 4 of the CM yield, the fraction of photoexcited NCs initially found in the BX state, $y_{cm} = p_2^o / (p_1^o + p_2^o)$,³⁴ were obtained as the ratio $y_{cm} = a_{BX}/a_X / (a_{BX}/a_X)_{\text{sat}}$ from fitting the uv-excited decays to the form $a_{BX} \exp(-t/\tau_{BX}) + a_X f(t)$.³¹

As seen in Fig. 4, our results do not match the $\hbar\omega/E_g$ dependence of y_{cm} found in TA measurements on CdSe NCs using 6.2 eV excitation¹² (Fig. 4). This could be because y_{cm} is not only a function of the ratio $\hbar\omega/E_g$, as suggested by TA on PbSe NCs,⁸ but also depends explicitly on $\hbar\omega$. However, our interpretation of recent tPL data at 6.2 eV (Ref. 19) using our estimated $k_{BX}^{\text{rad}} > 3k_X^{\text{rad}}$ suggests a y_{cm} of at most $\approx 35\%$ even at $\hbar\omega/E_g \approx 3.2$, instead of the 70% CM yield reported, which assumed $k_{BX}^{\text{rad}} = 2k_X^{\text{rad}}$.¹⁹ tPL and TA assessments of CM yield in CdSe NCs therefore appear to disagree, and it is possible that CM in semiconductor NCs is generally less efficient and not as universal as has been thought.

There are several reasons to expect a different CM en-

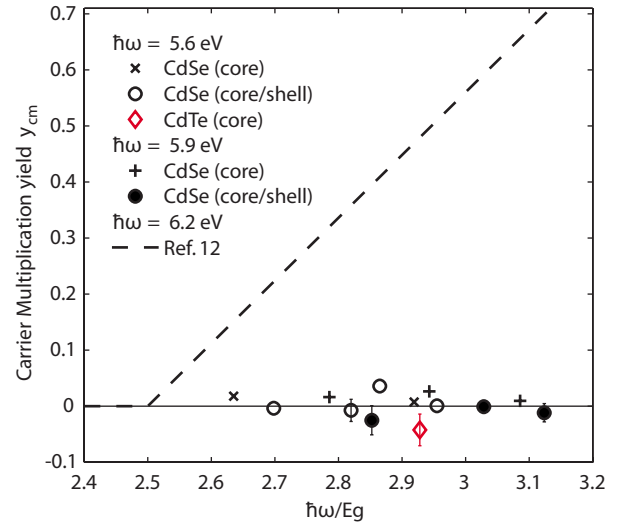


FIG. 4. (Color online) Carrier multiplication yields under 5.6 and 5.9 eV excitation extracted from tPL decays, $y_{cm} = a_{BX}/a_X / (a_{BX}/a_X)_{\text{sat}}$. Conservative (small) values $(a_{BX}/a_X)_{\text{sat}}$ were used for each sample. 2σ -wide error bars from repeated measurements are shown if larger than the symbols. The dashed line is the y_{cm} vs $\hbar\omega/E_g$ dependence found in the TA studies of Ref. 12 using $\hbar\omega=6.2$ eV.

hancement in II-VI semiconductors compared to the lead chalcogenides. The electronic state structure in wide gap NCs at energies $\geq 1E_g$ in excess of the band edge is likely bulklike with level spacings that are small. On the other hand, the analogous electronic states in the lead chalcogenides might be more discrete in character because of the smaller E_g and lighter effective masses. For these reasons, our experimental conclusions cannot be extended to the narrow band NCs, but the findings suggest the need to verify TA assessments of y_{cm} in the lead chalcogenides with other techniques such as tPL.

We note that the nature of a potential CM enhancement mechanism in NCs is itself not well understood. Although theoretical schemes have made progress towards explaining some of the reported phenomenology, these calculations have yet to quantitatively account for the balance of Coulomb and intraband relaxation processes leading to CM enhancement in a way that is clearly consistent with what is already known about carrier cooling and Auger rates in NCs. Calculations based on a traditional impact ionization model²⁶ reconcile fast CM (< 1 ps) with the slower band-edge Auger multiexciton relaxation (~ 100 ps) but make the assumption of constant Coulomb matrix elements between X and BX subspaces. While this “random- k ”-like approximation appears justified for the specific case of bulk Si at high energies,^{1,27} it might not apply to direct-gap semiconductor NCs, especially since the NC surface is thought to play a large role in Auger-like and other Coulomb processes.^{7,28} Other researchers have pursued a generalized treatment, going beyond the perturbative approach of typical impact ionization calculations to examine the effect of phase and population relaxation rates on the CM process.^{9,29} Calculations on PbSe NCs using a simple model of the electronic structure have shown efficient

CM (Ref. 29) but, in doing so, obtain large values of Coulomb matrix elements that appear to conflict with the much slower observed Auger rates. The third approach, virtual-state-mediated CM,¹¹ has so far not taken dephasing or population decay into account but could be generalized with the introduction of decay rates in the energy denominators of their second-order perturbation expression ($E \rightarrow E - i\Gamma$). All theoretical approaches so far thus hinge on the relative rates of Coulomb interaction and intraband relaxation at threshold, but neither has been measured or accurately calculated for NCs.

In summary, we have determined CM efficiencies in CdSe and CdTe NCs by transient photoluminescence. Exciton and biexciton features were first characterized under 3.1 eV excitation from which we find a relatively fast BX radiative rate

$k_{BX}^{\text{rad}} > 3k_X^{\text{rad}}$. Measurements under weak 5.6 and 5.9 eV excitation show no evidence of biexciton generation, and thus no CM, up to photon energies as high as $3.1E_g$.

This work was funded in part by the NSF MRSEC program (Grant No. DMR 0213282) at MIT and the authors made use of its Shared Experimental Facilities. It was also funded by the NSEC Program of the National Science Foundation (Grant No. DMR-0117795), the David and Lucile Packard Foundation, the Department of Energy (Contract No. DE-FG02-02ER45974), the Harrison Spectroscopy Laboratory (Contract No. NSF-CHE-011370), and the NSF-NIRT (Contract No. CHE-0507147). The authors would also like to thank Venda Porter, Scott Geyer, Numpon Insin, and Yintai Chan for help in sample preparations.

*mgb@mit.edu

- ¹M. Wolf, R. Brendel, J. H. Werner, and H. J. Queisser, *J. Appl. Phys.* **83**, 4213 (1998).
- ²D. Harrison, R. A. Abram, and S. Brand, *J. Appl. Phys.* **85**, 8186 (1999).
- ³W. Shockley and H. J. Queisser, *J. Appl. Phys.* **32**, 510 (1961).
- ⁴V. I. Klimov, *Appl. Phys. Lett.* **89**, 123118 (2006).
- ⁵A. J. Nozik, *Annu. Rev. Phys. Chem.* **52**, 193 (2001).
- ⁶D. Chepic, A. L. Efros, A. Ekimov, M. Ivanov, V. Kharchenko, I. Kudriavtsev, and T. Yazeva, *J. Lumin.* **47**, 113 (1990).
- ⁷L.-W. Wang, M. Califano, A. Zunger, and A. Franceschetti, *Phys. Rev. Lett.* **91**, 056404 (2003).
- ⁸R. D. Schaller and V. I. Klimov, *Phys. Rev. Lett.* **92**, 186601 (2004).
- ⁹R. J. Ellingson, M. C. Beard, J. C. Johnson, P. Yu, O. I. Micic, A. J. Nozik, A. Shabaev, and A. L. Efros, *Nano Lett.* **5**, 865 (2005).
- ¹⁰J. E. Murphy, M. C. Beard, A. G. Norman, P. Ahrenkiel, J. C. Johnson, P. Yu, O. I. Micic, R. J. Ellingson, and A. J. Nozik, *J. Am. Chem. Soc.* **128**, 3241 (2006).
- ¹¹R. D. Schaller, V. M. Agranovich, and V. I. Klimov, *Nat. Phys.* **1**, 189 (2005).
- ¹²R. D. Schaller, M. Petruska, and V. I. Klimov, *Appl. Phys. Lett.* **87**, 253102 (2005).
- ¹³P. Guyot-Sionnest, B. L. Wehrenberg, and D. Yu, *J. Chem. Phys.* **123**, 074709 (2005).
- ¹⁴B. L. Wehrenberg, C. J. Wang, and P. Guyot-Sionnest, *J. Phys. Chem. B* **106**, 10634 (2002).
- ¹⁵J. M. Harbold, H. Du, T. D. Krauss, K. S. Cho, C. B. Murray, and F. W. Wise, *Phys. Rev. B* **72**, 195312 (2005).
- ¹⁶V. I. Klimov, A. A. Mikhailovsky, D. W. McBranch, C. A. Leatherdale, and M. G. Bawendi, *Science* **287**, 1011 (2000).
- ¹⁷J. Michel Caruge, Y. Chan, V. Sundar, H. J. Eisler, and M. G. Bawendi, *Phys. Rev. B* **70**, 085316 (2004).
- ¹⁸C. Bonati, M.B. Mohamed, D. Tonti, G. Zgrablic, S. Haacke, F. van Mourik, and M. Chergui, *Phys. Rev. B* **71**, 205317 (2005).
- ¹⁹R. D. Schaller, M. Sykora, S. Jeong, and V. I. Klimov, *J. Phys. Chem. B* **110**, 25332 (2006).
- ²⁰G. Schlegel, J. Bohnenberger, I. Potapova, and A. Mews, *Phys. Rev. Lett.* **88**, 137401 (2002).
- ²¹B. R. Fisher, H. J. Eisler, N. E. Stott, and M. G. Bawendi, *J. Phys. Chem. B* **108**, 143 (2004).
- ²²B. R. Fisher, J.-M. Caruge, D. Zehnder, and M. G. Bawendi,

Phys. Rev. Lett. **94**, 087403 (2005).

- ²³M. Nirmal, D. J. Norris, M. Kuno, M. G. Bawendi, A. L. Efros, and M. Rosen, *Phys. Rev. Lett.* **75**, 3728 (1995).
- ²⁴A. L. Efros, M. Rosen, M. Kuno, M. Nirmal, D. J. Norris, and M. Bawendi, *Phys. Rev. B* **54**, 4843 (1996).
- ²⁵J. Shumway, A. Franceschetti, and A. Zunger, *Phys. Rev. B* **63**, 155316 (2001).
- ²⁶A. Franceschetti, J. An, and A. Zunger, *Nano Lett.* **6**, 2191 (2006).
- ²⁷E. O. Kane, *Phys. Rev.* **159**, 624 (1967).
- ²⁸A. L. Efros, in *Semiconductor Nanocrystals, from Basic Principles to Applications*, edited by A. L. Efros, D. J. Lockwood, and L. Tsybeskov (Kluwer, New York, 2003).
- ²⁹A. Shabaev, A. L. Efros, and A. J. Nozik, *Nano Lett.* **6**, 2856 (2006).
- ³⁰At very high excitation fluence we do observe an additional very fast component but its dynamics appear consistent with 1S-1S emission from higher multiexcitonic states. The impact of this feature on further analysis was minimized by omitting early time ($t \lesssim \frac{1}{2}\tau_{BX}$) data from fitting.
- ³¹See EPAPS Document No. E-PRBMDO-76-R08732 for details on experimental and analysis methods. For more information on EPAPS, see <http://www.aip.org/pubservs/epaps.html>
- ³²For our approximately Gaussian beam profiles, $p_{m>0}^o$ transitions from $\sim n_0$ to $\sim \ln n_0$ instead of fully saturating, and the ratio $p_{m>1}^o/p_{m>0}^o$ is much smaller and more slowly approaches unity than for uniform illumination. Our fits neglect the last term in the expression for a_{BX} which accounts for the small delaying effect of cascade from higher multiexcitons ($k > 2$). This approximation leads to at most a $\approx 25\%$ overestimate of $(a_{BX}/a_X)_{\text{sat}}$ and has been taken into consideration in our final CM analysis (Ref. 31).
- ³³Concentrated (OD ~ 1 at 3.1 eV), stirred samples and short integration times were employed to minimize exposure at 5.6 eV. Prolonged exposure leads to irreversible degradation reflected in emission quenching and faster, more strongly multiexponential X dynamics, which were monitored throughout the experiment to verify sample integrity.
- ³⁴It has been common in the literature to report CM yields in terms of an exciton internal quantum efficiency (IQE), which is related to our y_{cm} by $\text{IQE} = 100\% (y_{\text{cm}} + 1)$.